Edinburgh Research Explorer

Sodium homeostasis is preserved in a global 11β-hydroxysteroid dehydrogenase type 1 knockout mouse model

Citation for published version:
Christensen, TH, Bailey, MA, Kenyon, CJ, Jensen, BL & Hunter, RW 2015, 'Sodium homeostasis is preserved in a global 11β-hydroxysteroid dehydrogenase type 1 knockout mouse model', *Experimental physiology*, vol. 100, no. 11, pp. 1362-78. https://doi.org/10.1113/EP085177

Digital Object Identifier (DOI):
10.1113/EP085177

Link:
Link to publication record in Edinburgh Research Explorer

Document Version:
Peer reviewed version

Published In:
Experimental physiology

Publisher Rights Statement:
This is the peer reviewed version of the article, which has been published in final form at http://onlinelibrary.wiley.com/doi/10.1113/EP085177/abstract;jsessionid=2731CE63350D5837F31553C05BADEC00.f03t03. This article may be used for non-commercial purposes in accordance with Wiley Terms and Conditions for Self-Archiving.

General rights
Copyright for the publications made accessible via the Edinburgh Research Explorer is retained by the author(s) and / or other copyright owners and it is a condition of accessing these publications that users recognise and abide by the legal requirements associated with these rights.

Take down policy
The University of Edinburgh has made every reasonable effort to ensure that Edinburgh Research Explorer content complies with UK legislation. If you believe that the public display of this file breaches copyright please contact openaccess@ed.ac.uk providing details, and we will remove access to the work immediately and investigate your claim.

Download date: 04. Jun. 2024

Title Page

Title:

Sodium homeostasis is preserved in a global 11β-hydroxysteroid dehydrogenase type 1 knockout mouse model

Authors:

Thorbjørn H. Christensen[1, 2], Matthew A. Bailey[1], Christopher J. Kenyon[1], Boye L. Jensen[2] & Robert W. Hunter[1]

Affiliations:

1) University/BHF Centre for Cardiovascular Science, University of Edinburgh, Edinburgh, United Kingdom

2) Department of Cardiovascular and Renal Research, University of Southern Denmark, Odense, Denmark

Corresponding author:

Robert W. Hunter; robert.hunter@ed.ac.uk; University of Edinburgh / BHF Centre for Cardiovascular Science, Room W3.33B, The Queen's Medical Research Institute, 47 Little France Crescent, Edinburgh EH16 4TJ, United Kingdom

Running title:	Sodium homeostasis in the Hsd11b1 null mouse
Key words:	11βHSD1; glucocorticoid; sodium
Number of words:	5380 (excluding references and figure legends)
Number of references:	35
Subject Area:	Renal physiology

This is an Accepted Article that has been peer-reviewed and approved for publication in the Experimental Physiology, but has yet to undergo copy-editing and proof correction. Please cite this article as an Accepted Article; doi: 10.1113/EP085177 .

New Findings

- *What is the central question of this study?*

Glucocorticoids act in the kidney to promote salt and water retention. Renal 11β-hydroxysteroid dehydrogenase type 1, by increasing local concentrations of glucocorticoids, may exert an anti-natriuretic effect. We hypothesised that global deletion of 11β-hydroxysteroid dehydrogenase type 1 in the mouse would give rise to a salt-wasting renal phenotype.

- *What is the main finding and its importance?*

We subjected a mouse model of global 11βHSD1 deletion to studies of water and electrolyte balance, renal clearance, urinary steroid excretion, renin-angiotensin system activation and renal sodium transporter expression. We found no significant effects on renal sodium or water excretion. Any effect of renal 11βHSD1 on sodium homeostasis is subtle.

Abstract

Glucocorticoids act in the kidney to regulate glomerular haemodynamics and tubular sodium transport; the net effect favours sodium retention. 11β-hydroxysteroid dehydrogenase type 1 (11βHSD1) is expressed in the renal tubules and the interstitial cells of the medulla, where it is likely to regenerate active glucocorticoids from inert 11-keto forms. The physiological function of renal 11βHSD1 is largely unknown. We hypothesised that loss of renal 11βHSD1 would result in salt wasting, and tested this in a knockout mouse model in which 11βHSD1 was deleted in all body tissues. In balance studies, 11βHSD1 deletion had no effect on water, sodium or potassium metabolism; transition to a low sodium diet did not reveal a natriuretic phenotype. Renal clearance studies demonstrated identical haemodynamic parameters (arterial blood pressure, renal blood flow, glomerular filtration rate) in knockout and wild-type mice, but revealed an augmented kaliuretic response to thiazides in 11βHSD1 knockouts. There was no effect on the natriuretic response to the amiloride analogue benzamil. Urinary excretion of deoxycorticosterone (DOC) was higher in 11βHSD1 knockout mice and there was hypertrophy of cells in the zona fasciculata of the adrenal cortex. There was no difference in the activity of the renin-angiotensin and nitric oxide systems, no difference in renal histology, and no difference in the abundance of key tubular transporter proteins. We conclude that any effect of 11βHSD1 on renal sodium excretion is subtle.

Introduction

In the adult mammalian kidney, glucocorticoids regulate tissue haemodynamics (increasing renal blood flow and glomerular filtration rate), the production of vasoactive paracrine / endocrine factors and sodium transport in the renal tubule (Mangos *et al.*, 2003; Hunter *et al.*, 2014*b*). These renal effects contribute to the regulation of total body sodium and systemic arterial blood pressure (ABP).

In target tissues, glucocorticoid activity is determined by the density of nuclear glucocorticoid receptors (GR), circulating levels of glucocorticoids and the activity of 11β-hydroxysteroid dehydrogenase (11βHSD) enzymes. 11βHSD1 regenerates active glucocorticoids, catalysing the conversion of cortisone to cortisol in humans (11-dehydrocorticosterone to corticosterone in rodents); 11βHSD2 catalyses the reverse reaction (Chapman *et al.*, 2013). Adipose-specific 11βHSD1 deletion in the mouse attenuates the metabolic consequences of circulating glucocorticoid excess, demonstrating that 11βHSD1 activity is a major regulator of local glucocorticoid activity, at least in adipose tissue (Morgan *et al.*, 2014).

Both 11βHSD1 and 11βHSD2 are expressed in the kidney. 11βHSD2 is expressed in the tubular cells of the distal renal tubule (connecting tubule and collecting ducts), where it prevents active glucocorticoids from binding and activating the mineralocorticoid receptor (MR). MR can bind glucocorticoids and mineralocorticoids with high affinity *in vitro* (Arriza *et al.*, 1987); 11βHSD2 thus acts to maintain the specificity of aldosterone-MR signalling *in vivo*. 11βHSD1 is expressed in the proximal tubule, macula densa and the interstitial cells of the renal medulla (Odermatt & Kratschmar, 2012); its *in vivo* function at these sites is controversial. Enzyme kinetic studies using homogenised kidney preparations suggest that 11βHSD1 may act as a dehydrogenase (i.e. converting cortisol to cortisone) (Gong *et al.*, 2008). However, siRNA-mediated knock-down of 11βHSD1 activity in the renal medulla results in reduced urinary excretion of corticosterone (Liu *et al.*, 2008), consistent with the enzyme operating as a reductase *in vivo* (i.e. regenerating active glucocorticoid).

The downstream physiological consequences of renal 11βHSD1 activity are largely unknown. However, two lines of evidence suggest that renal 11βHSD1 activity influences systemic blood pressure in rodents. First, renal 11βHSD1 mRNA expression is higher in a salt-sensitive rat model (Dahl SS) than in a salt-resistant consomic strain (SS-13^{BN}/Mcw). This positive association between renal 11βHSD1 activity and systemic blood pressure is only apparent when the animals receive high dietary salt (Liang *et al.*, 2003; Liu *et al.*, 2008). Second, knockdown of Hsd11b1 mRNA in the renal medulla of Dahl SS rats attenuates salt-sensitive hypertension (Liu *et al.*, 2008), providing the most compelling evidence for a causal link between renal 11βHSD1 activity and blood pressure. Moreover, the renal expression of 11βHSD1 is modified by dietary sodium intake, implying that its activity may be regulated by factors directed at maintaining sodium homeostasis. High dietary sodium reduces Hsd11b1 mRNA expression in rat proximal tubules (McKinnell *et al.*, 2000) and in the renal medulla of salt-resistant rats (Liang *et al.*, 2003; Liu *et al.*, 2008).

The literature therefore suggests that renal 11βHSD1 activity leads to increased systemic blood pressure, although the mechanism remains unknown. Given that glucocorticoids can stimulate sodium reabsorption in the proximal nephron, distal nephron and collecting ducts (Hunter *et al.*, 2014*b*), we hypothesised that renal 11βHSD1 activity opposes natriuresis by regenerating active glucocorticoid in the renal tubules. It follows that the global deletion of 11βHSD1 would result in a tendency to renal sodium loss, manifesting in a phenotype that would be subject to neurohormonal compensation from the RAAS, hypothalamo-pituitary-adrenal (HPA) axis, sympathetic nervous system and other natritropic regulators.

The aim of this study was to assess the effect of global 11βHSD1 deletion on renal sodium transport and to determine the implicated neurohormonal / transport systems. We subjected 11βHSD1 knockout mice to perturbations in dietary sodium intake and examined the consequences for systemic sodium and water homeostasis, renal haemodynamics, renal sodium transport pathways and systemic steroidogenesis.

Methods

Ethical approval

All experimental procedures were performed under UK Home Office licence in accordance with the Animals (Scientific Procedures) Act, 1986. All experimental procedures involving live animals were reviewed and approved by local veterinary surgeons.

Hsd11b1$^{-/-}$ and wild-type mice

Mice had free access to water and a standard RM1 diet (0.25% Na^+; Special Diet Services, Witham, UK) unless otherwise stated, and were maintained on a 12 hour light-dark cycle. Wild type control mice (C57BL/6J) were obtained from an in-house colony, derived from purchased stock (Harlan Laboratories, Loughborough, UK). Male mice were used for all experiments. Hsd11b1$^{-/-}$ mice were the offspring of homozygous-homozygous crosses in a colony carrying a null mutation in the Hsd11b1 gene on the C57BL/6J background (Morton *et al.*, 2004). The gene mutation (originally introduced on an MF1 background) has been previously shown to completely ablate 11βHSD1 activity *in vivo* and *in vitro* (Kotelevtsev *et al.*, 1997).

Balance studies

Mice were housed individually in metabolic cages that enabled the independent collection of urine and faeces and were left to acclimatise for five days before any experimental data were obtained. Drinking water and diet were provided *ad libitum*. Animals were given gel diets to minimise diet dispersion and sample contamination. Gel diet production was adapted from an existing method (Ahn *et al.*, 2004). Diets contained 36% ground diet (RM1; or low sodium diet, Ziegler Bros, Gardners, PA, USA), 3.8% bovine gelatine (Dr. Oetker Nahrungmittel, Bielefeld, Germany) and supplementary NaCl to make 0.026% Na^+ (low-), 0.2% Na^+ (normal-) and 2.1% Na^+ (high-) sodium diets (percentages in dry weight equivalents). Following acid digestion, the Na^+ content of each diet was verified by flame photometry.

During the study period, mice received control Na^+ diet for 4 days and then either high or low Na^+ diet for 8 days (Figure 1A). Dietary intake, urine output and faecal output were measured over 24 hour collection periods, each finishing immediately after the nocturnal active period. At the end of the study period, animals were sacrificed by cervical dislocation and terminal blood and kidneys were snap-frozen and stored at – 80°C.

Faecal samples were dried at 105°C for 24 hours to assess gastrointestinal water losses. To measure faecal Na^+ and K^+ content, dried faecal samples were homogenised then digested in concentrated nitric acid (~15M; Fisher Scientific) for 24 hours at 65°C in an orbital shaker. Digested faecal and urine samples were diluted in 10 ppm diluent concentrate (1% Brij35, BWB Technologies UK, Braintree, UK) 1:6 and 1:25-1:50, respectively before measurement of [Na^+] and [K^+] by flame photometry (BWB Technologies UK).

Results were normalised to kidney weight (rather than body weight) because $Hsd11b1^{-/-}$ mice differ from wild-types in their adipose tissue distribution (Morton *et al.*, 2004).

Renal clearance

Renal clearance experiments were performed under terminal anaesthesia (Inactin, thiobutabarbital sodium salt hydrate, Sigma) as previously described (Hunter *et al.*, 2014*a*). Anaesthesia was induced with an intraperitoneal injection of c. 150 mg per kg body weight and maintained by repeated intravenous bolus injection at a level sufficient to suppress the blink reflex and a motor response to toe pinch (typical total dose 200 – 250 mg per kg body weight). Catheters were inserted into the trachea, jugular vein, carotid artery and bladder. A bolus dose (0.1 ml / 10 g body weight) of physiological saline solution was given via the jugular catheter as soon as intravenous access was established, followed by a continuous infusion of 0.2 ml / 10 g / hour with a solution containing (in mM): 146 Na^+, 5 K^+, 113 Cl^-, 15 HCO_3^- and (in % w/v) 0.25 FITC-inulin, 0.5 PAH (p-Aminohippuric acid sodium salt, Sigma), pH 7.4. Mean arterial blood pressure was recorded from the carotid catheter in real time.

Urine and blood samples were collected according to the protocol depicted in Figure 1B. Mice were left to equilibrate for 60 minutes after surgery. Urine was collected over a 40-minute baseline period, then an intravenous bolus dose of diuretic (either bendroflumethiazide or benzamil) at a dose of 2 mg per kg body weight in 1% DMSO was administered. A 20-minute period of re-equilibration was followed by a second 40-minute urine collection. ~70 μl blood samples were obtained from the arterial line at the end of the first equilibration period and after each urine collection; these were used to determine haematocrit, plasma [inulin] and [PAH]. At the end of the protocol, a 1 ml sample of blood was obtained for the measurement of plasma [Na^+], [K^+] and [Cl^-]. The surgeon was blinded to genotype until after all analyses were completed.

The inulin, PAH and electrolyte assays were conducted as previously described (Hunter *et al.*, 2014*a*). Briefly, [FITC-inulin] in plasma and urine was determined by measuring fluorescence intensity at pH 7.4, relative to a 9-point standard curve in duplicate. [PAH] in plasma and urine was determined by a colorimetric method, relative to an 11-point standard curve in duplicate. [Na^+], [K^+] and [Cl^-] were measured by an ion-sensitive electrode (Roche 9180 Electrolyte Analyzer). Glomerular filtration rate (GFR), effective renal blood flow (eRBF) and the fractional excretion of electrolytes (FE_{Na}, FE_K, FE_{Cl}) were derived from inulin and PAH clearance, using standard equations (Hunter *et al.*, 2014*a*).

Urinary steroid and NOx analysis

Urinary corticosterone, aldosterone and deoxycorticosterone (DOC) were measured by colorimetric ELISA as previously described (Al-Dujaili *et al.*, 2009*b*, 2009*a*). Briefly, urinary steroids were extracted in surplus 2-methoxy-2-methylpropane and re-constituted in assay buffer. 96-well plates were coated with steroid-albumin conjugates overnight (1.25 μg / ml; Steraloids, Newport, RI, USA). The following reagents were then added in sequence (with intermediate washing steps): blocking buffer, standards in duplicate, samples in duplicate, primary antibody (sheep anti-aldosterone at 1:30000; sheep anti-corticosterone at 1:20000 or rabbit anti-DOC at 1:20000, produced in-house), HRP-linked secondary antibody (donkey anti-sheep Ig at 1:11000 or goat anti-rabbit at 1:11000, Sigma), substrate solution and stop solution. Absorbance was measured at 450 nm.

The concentration of total urinary nitrite and nitrate (NOx) was measured by colorimetric assay (780001, Cayman Chemicals, Ann Arbor, MI, USA), according to the manufacturer's instructions after diluting urine 1:60.

Renin and angiotensinogen radioimmunoassay

Renin and angiotensinogen concentrations were measured by radioimmunoassay of angiotensin I generated by incubating plasma with excess angiotensinogen substrate (for renin assay) or excess renin enzyme (for angiotensinogen measurements). Plasma samples (diluted tenfold with assay buffer for angiotensinogen), with added substrate or enzyme, were incubated with angiotensin I antibody at 37 or 0 °C for 1 hour before the addition of ice-cold assay buffer. Duplicate angiotensin I standards (11 points, 0-40ng/L) were incubated in parallel. Sample and standard assay tubes were then equilibrated at 2 °C for 48 hours with added ^{125}I angiotensin (PerkinElmer). Free and bound angiotensin were separated by charcoal extraction and radioactivity in the free fraction was counted in a Wallac gamma counter. Renin enzyme and angiotensinogen substrate were prepared from cytosolic extracts of mouse submandibular glands and from the plasma of nephrectomised rats respectively. Results were expressed as the difference in angiotensin I values in tubes incubated at 37 and 0 °C.

Histology

Kidneys were fixed *in situ* by perfusion fixation as previously described (Hunter *et al.*, 2014*c*). Mice were sacrificed by vascular perfusion under terminal anaesthesia (sodium pentobarbital, Sagatal; Ceva Santé Animale, Libourne, France; 50 mg per kg body weight as an intra-peritoneal bolus). The infra-renal aorta was cannulated to permit retrograde perfusion with a vent in the vena cava. 10 ml heparinised saline (20 units / ml in PBS) were infused followed immediately by 50 ml fixative (fresh 4 % PFA in PBS, pH 7.4), delivered at a rate of 15 ml / min by a Gilson Minipuls 3 peristaltic pump. The kidneys was removed, the poles cut off and discarded, and the central portion immersed in 4 % PFA at 4°C for 24 hours before being embedded in paraffin wax. 5 micron sections were cut in the transverse plane and either stained with haematoxylin-eosin or used for immunohistochemistry.

Immunohistochemistry (detection of NCC)

Tissue sections were de-waxed and hydrated through graded alcohols and then heated in the presence of 10 mM citrate, pH 6.0. Indirect immunofluorescent detection of NCC was performed using rabbit anti-NCC (Millipore, AB3553) at 1:1000 dilution, with a biotinylated secondary antibody (swine anti-rabbit IgG, DAKO) at 1:250. The binding sites of secondary antibodies were detected using a Streptavidin-HRP amplification step (Vectastain R.T.U. Elite ABC reagent) and DAB (3,3'-diaminobenzidine).

Analysis of adrenal cell size

Adrenals were collected from mice housed in metabolic cages. After formalin fixation and careful dissection (to remove surrounding adipose tissue), they were embedded in paraffin blocks, sectioned and stained with haematoxylin and eosin. Sections were analysed with a Zeiss Axioskop compound microscope using a Nikon Coolpix 995 camera and MCID imaging software. Cross-sectional areas of cells in morphologically distinct regions of the cortex and medulla were estimated by counting the number of nuclei (150-200) in a defined field area. The observer was blinded to genotype and dietary Na^+ treatment. Results were expressed as mean ± standard error of averages from triplicate measurements of sections from four adrenal glands / treatment group.

Western blot analysis

Kidneys were homogenised in a buffer containing phosphatase, kinase and protease inhibitors (250 mM sucrose,10 mM triethanolamine, 2 mM EDTA, 50 mM NaF, 25 mM Na β-glycerophosphate, 5 mM Na pyrophosphate, 1 mM Na orthovanadate, 1 % Protease Inhibitor Cocktail Set III, Calbiochem®, pH 7.6). Supernatants from two 15 minute centrifugations at 4000 *g* were pooled to form a total cellular protein fraction free from gross cellular and nuclear debris. Total protein concentration was measured using a commercial bicinchonic acid assay (Pierce/Thermo Scientific, Rockford, IL, USA).

For high molecular weight protein targets (>100 kDa), protein samples were diluted in NuPAGE LDS sample buffer (Invitrogen/Life Technologies, Paisley, UK) and 50 mM dithiothreitol (DTT; Sigma). After heating to 70°C for 15 mins, samples were loaded in NuPAGE Novex 3-8% Tris-Acetate gels (Invitrogen/Life Technologies) and electrophoresed for 75 min at 150 V. For lower molecular weight targets, samples were diluted in Laemmli buffer and (after heating) loaded in 12% Precise Protein Gels (Pierce/Thermo Scientific) and electrophoresed for 65 min at 100 V.

Samples were transferred to a PVDF membrane (Hybond P, GE Healthcare Life Sciences, Little Chalfont, UK) using semi-dry transfer cell (Bio-Rad Laboratories Ltd, Hemel Hempstead, UK) at 10V for 30 min. Membranes were incubated with blocking buffer (5 % w/v non-fat dry milk powder / 0.2 % v/v Tween-20 in PBS) on a rolling shaker at room temperature for 1 hr and then incubated with primary antibody overnight at 4°C. Primary antibodies and their dilutions were: rabbit anti-NCC (Millipore, AB3553) at 1:1000; sheep anti-pT53-NCC (Division of Signal Transduction Therapy, Dundee University), at 1:500 (= 0.2 – 1.2 μg / ml); sheep anti-NKCC2 (DSTT, Dundee) at 1:10000; rabbit anti-ENaC-γ (Johannes Loffing, Zurich) at 1:5000; sheep anti-NDRG1 (DSTT, Dundee) at 1:515; sheep anti-pNDRG1 (DSTT, Dundee) at 1:150. For Western blots designed to recognise pT53-NCC, the corresponding non-phosphorylated peptide was included in the solution of primary antibody at a final concentration of 10μg / ml. After three five-minute washes with wash buffer (0.2 % v/v Tween-20 in PBS) the membrane was incubated with an HRP-conjugated secondary antibody for 1 – 2 hrs at room temperature and then washed again (three ten-minute washes). Secondary antibodies and their dilutions were: goat anti-rabbit IgG-HRP (Santa-Cruz, sc-2030) at 1:2000; donkey anti-sheep IgG-HRP (Sigma, A3415) at 1:20000. Peroxidase activity was revealed using SuperSignal® West Pico Chemiluminescent Substrate to expose photographic film.

Films were photographed using a digital SLR camera (Nikon D40) with the exposure set to maximise dynamic range without significant pixel saturation. Images were analysed in ImageJ (version 1.47v). A rectangular region of interest (ROI) was drawn to encompass the entire vertical range of each lane and the area under this curve was taken as a measure of the band density. No background subtraction step was applied. The bottom portion of each gel was excised prior to transfer to the PVDF membrane and stained with Coomassie blue. The density of each lane on the film was divided by the density of the corresponding Coomassie lane in order to correct for variation in the total amount of protein loaded for each sample. The final data were normalised so that for each assay, the wild-type group had a mean value of 1.0.

Statistical analysis

Data were assessed for Gaussian distribution using D'Agostino & Pearson omnibus test or Shapiro-Wilk normality tests (for small n-numbers). Analysis was carried out using unpaired Student's t-test or 2-way ANOVA (with repeated measures) with Holm-Šídák *post hoc* test as appropriate on GraphPad Prism 6.0 Software. $P < 0.05$ was considered significant. Results are presented as ANOVA-derived p-values and mean ± 95 % confidence interval (CI) unless otherwise specified.

Results

Urinary electrolyte excretion in conscious Hsd11b1$^{-/-}$ and wild-type mice

Net urinary electrolyte excretion was measured in conscious mice housed in metabolism cages. After acclimatisation and baseline measurements (on 0.2% Na^+ diet), animals were transitioned to either high (2.1%) or low (0.026%) dietary sodium (Figure 1A). Baseline characteristics are summarised in Table 1. Hsd11b1$^{-/-}$ mice had significantly higher body weight and kidney weight, compared to age-matched wild-type. Heart weights did not differ between genotypes (wild-type: 127.1 – 230.5 mg vs. Hsd11b1$^{-/-}$ 149.8 – 178.8 mg; n=7/8; 95%CI; p=0.650 by unpaired t-test).

Dietary intake of food and water did not differ significantly between genotypes (the p-values for comparison between genotypes by 2-way ANOVA were as follows: in the low-Na^+ cohort, $p = 0.395$ for water intake and $p = 0.234$ for food intake; in the high-Na^+ cohort, $p = 0.428$ for water intake and $p = 0.208$ for food intake). Any variation in the balance data was dominated by changes in excretion of water, Na^+ or K^+ (raw data provided in Supplemental Table S1).

$Hsd11b1^{-/-}$ mice did not differ from wild-type controls in water balance, Na^+ balance or K^+ balance under basal conditions. Nor were there any differences in their response to either dietary Na^+ loading or restriction (Figure 2). In the low-Na^+ study (n = 12), $Hsd11b1^{-/-}$ mice had reduced insensible losses of water and K^+ (manifesting as a smaller positive 24 hr balance) under baseline conditions. However, these differences were not replicated in the statistically more powerful (n = 22) high-Na^+ study. Following transition to a high-Na^+ diet, in both genotypes there was a transient period of positive Na^+ balance during the first 4 days, until Na^+ excretion was up-regulated to match intake (Figure 2B).

Renal clearance under anaesthesia

In order to resolve glomerular and tubular effects, renal function was investigated by renal clearance under terminal anaesthesia, in mice that had been maintained on a normal (0.2%) Na^+ diet. Haemodynamic parameters (arterial blood pressure, ABP; renal blood flow, RBF; glomerular filtration rate, GFR), plasma electrolyte concentrations and urinary electrolyte excretion were measured at baseline (after an initial acclimatisation period) and after a bolus dose of bendroflumethiazide (BFTZ, 2 mg per kg body weight; Figure 1B). BFTZ is an inhibitor of the NaCl co-transporter (NCC) in the distal convoluted tubule (DCT), a known target of glucocorticoid signalling (see discussion).

$Hsd11b1^{-/-}$ mice did not differ from wild-types in either the concentration of Na^+, K^+ and Cl^- in the plasma (Table 2). There were no significant genotype-specific differences in ABP, RBF and GFR either at baseline or following BFTZ, although there was a trend towards lower RBF and lower GFR in the $Hsd11b1^{-/-}$ mice at baseline (Figure 3). The was no significant difference in heart weight between the two genotypes. Urinary Na^+ and Cl^- excretion both exhibited the expected increase following thiazide administration, but there were no differences between this response in $Hsd11b1^{-/-}$ mice compared to wild-types, whether assessed as net urinary excretion ($U_{Na}V$ / $U_{Cl}V$) or as fractional excretion (FE_{Na}, FE_{Cl}) (Table 2B; Figure 3). BFTZ induced a kaliuresis of greater magnitude in $Hsd11b1^{-/-}$ mice than in wild-types ($p < 0.05$; Table 2B).

It is possible that the greater thiazide-induced kaliuresis in Hsd11b1$^{-/-}$ mice was the result of enhanced Na^+ reabsorption in the distal nephron through the epithelial sodium channel, ENaC. We therefore tested the effect of the ENaC inhibitor benzamil under renal clearance (Figure 1B). This elicited a natriuresis that was no different in Hsd11b1$^{-/-}$ and wild-type mice (Figure 4).

Urinary steroid excretion and adrenal morphology

We sought to determine the consequences of global 11βHSD1 loss for urinary steroid excretion. Urine samples collected from the metabolic studies were used make a longitudinal assessment of steroid excretion. There were no consistent genotype-specific differences in the urinary excretion of corticosterone or aldosterone (Figure 5). As expected, aldosterone excretion was inversely correlated with dietary Na^+ intake in both genotypes. DOC (deoxycorticosterone) excretion was elevated approximately 2-fold in Hsd11b1$^{-/-}$ mice; this difference was accentuated by high dietary Na^+, which elevated DOC excretion in both genotypes (Figure 5C).

Hsd11b1$^{-/-}$ mice also exhibited a difference in adrenal morphology (Figure 6). Compared to wild-types, cells of the zona fasciculata (ZF) were larger in Hsd11b1$^{-/-}$ mice – an effect most pronounced in the inner ZF (i.e. that part closest to the medulla). No differences were apparent in the zona glomerulosa or in the adrenal medulla.

Renin-angiotensin and nitric oxide systems

There were no genotype-specific differences in the plasma concentrations of renin and angiotensinogen (AGT). As expected, both compounds were suppressed by high dietary Na^+ feeding (Figure 7AB). Urinary excretion of nitrite and nitrate (NOx) varied in proportion to dietary Na^+ intake; there were no genotype-specific differences (Figure 7CD).

Gross renal structure and histology

There was no difference in the ratio of kidney to body weight between genotypes: 4.9 ± 0.4 in WT vs. 5.3 ± 0.4 in Hsd11b1$^{-/-}$ (mg kidney weight per g body weight; mean ± SD; n=13; p=0.11 by unpaired Student's t-test). Kidneys were fixed *in situ* by vascular perfusion, sectioned and stained with haematoxylin/eosin. There were no gross differences in renal histology between genotypes (Figure 8AB). There was no evidence of chronic kidney disease (e.g. glomerulosclerosis, interstitial fibrosis, tubular atrophy) in Hsd11b1 mice$^{-/-}$; nor was there any apparent expansion or atrophy of specific nephron segments. We applied an immunohistochemical stain (anti-NCC) to label the distal convoluted tubule, as this segment is known exhibit structural plasticity in response to perturbations in Na^+ homeostasis; the DCT appeared morphologically normal in Hsd11b1 mice$^{-/-}$ (Figure 8C-F). NCC was associated with the apical membranes of DCT cells and displayed no major difference in distribution or intensity between genotypes.

Expression of tubular transporter proteins

The abundance of key transporter proteins in whole kidney homogenates was determined by Western blot. We applied this analysis to mice maintained on normal dietary Na$^+$ and following dietary Na$^+$ restriction, as our over-arching hypothesis was that Hsd11b1$^{-/-}$ mice have a tendency to renal salt-wasting. We reasoned therefore that any perturbation in renal Na$^+$ homeostasis would be most pronounced following Na$^+$ depletion.

We analysed two tubular sodium transporters known to be regulated by glucocorticoids (the Na-K-2Cl co-transporter NKCC2 and NCC). In the case of NCC, in addition to measuring the abundance of total protein, we measured that of a phosphorylated form that is associated with active NaCl transport (pT53-NCC). There were no genotype-specific differences in the abundance of NKCC2, total NCC or pT53-NCC in kidneys harvested from mice maintained on a normal (0.2%) or low (0.026%) Na$^+$ diet (Figure 9).

Prompted by our finding of enhanced thiazide-induced kaliuresis in Hsd11b1$^{-/-}$ mice, we measured the abundance and predominant molecular mass of the gamma subunit of ENaC (ENaC-γ). Channel activation is associated with cleavage of this subunit from a form that runs at c. 85 kDa on Western blot to one that runs at c. 70 kDa (Masilamani *et al.*, 2002). As expected, the 70 kDa band was stronger in mice maintained on a low Na$^+$ diet. However there was no difference in the total abundance of ENaC-γ (assessed by densitometry of all bands), nor in the abundance of the 85 kDa or 70 kDa isoforms in Hsd11b1$^{-/-}$ compared to wild-type mice on either diet (Figure 9).

We also analysed the phosphorylation status of NDRG1 (n-myc downstream-regulated gene 1), an index of Sgk1 activity, itself a direct target of glucocorticoid signalling (Murray *et al.*, 2004; Inglis *et al.*, 2009). This was no different in the kidneys of Hsd11b1$^{-/-}$ mice, compared to wild-types (on either a normal or low Na$^+$ diet; Figure 9).

Discussion

Our primary hypothesis was that Hsd11b1$^{-/-}$ mice would display a propensity for renal Na$^+$ and water loss, as a consequence of diminished glucocorticoid generation in the kidney. The control of renal Na$^+$ excretion is dominated by the RAAS, with glucocorticoids playing a modulatory role (Hunter *et al.*, 2014*b*). Therefore we anticipated that any phenotype would be subtle, and subject to compensatory changes in other natritropic neurohormonal control systems.

Systemic and renal steroid metabolism

We found increased urinary excretion of DOC in Hsd11b1 mice$^{-/-}$, but excretion of corticosterone did not differ from wild-type mice. DOC is a precursor of corticosterone, and both steroids are synthesised in the zona fasciculata under the control of ACTH (Al-Dujaili *et al.*, 2009*b*). Circulating levels of DOC and corticosterone thus usually increase or decrease in parallel. We found cell hypertrophy in the zona fasciculata of Hsd11b1$^{-/-}$ adrenal, consistent with increased production of DOC and / or corticosterone. Circulating [corticosterone] is known to be elevated approximately 2-fold in Hsd11b1$^{-/-}$ mice (Kotelevtsev *et al.*, 1997; Morton *et al.*, 2004). As has been argued before, this is presumably a result of a loss of normal 11βHSD1 activity in the hypothalamus and pituitary, blunting the negative feedback effect of circulating glucocorticoids on ACTH production (Kotelevtsev *et al.*, 1997; Harris *et al.*, 2001). Human patients with genetic mutations inducing functional 11βHSD1 deficiency also exhibit excessive ACTH-mediated adrenal steroid secretion, with consequent hyperandrogenism (Lavery *et al.*, 2013).

Urinary excretion of corticosterone will reflect circulating [corticosterone] and the combined activities of renal 11βHSD1 and 11βHSD2. Our finding (that there is no difference in urinary excretion, despite evidence of increased corticosterone production) is compatible with the expected reduction in renal 11βHSD1 activity (assuming no difference in renal 11βHSD2). The urinary excretion of corticosterone is diminished following the inhibition of renal 11βHSD1 in rat kidneys (Liu *et al.*, 2008).

Renal electrolyte excretion: net effects

No significant urinary Na$^+$ losses were observed in Hsd11b1$^{-/-}$ mice – even when mice were transitioned to a low Na$^+$ diet. It is possible that no effect was seen because the elevated levels of circulating corticosterone compensated completely for absent renal 11βHSD1 activity, resulting in normal tissue levels of active glucocorticoid in the kidneys of Hsd11b1$^{-/-}$ mice. Furthermore, any natriuretic tendency may have been offset by increased mineralocorticoid activity from DOC (see below). We found no differences in measures of RAAS and NO system activity in Hsd11b1$^{-/-}$ mice, arguing against any major compensatory adjustment in these regulators of vascular tone, renal Na$^+$ excretion and ABP.

It is possible that our metabolic cage data were subject to confounding stress effects. We included a 5-day acclimatisation period, which should provide sufficient time for the stabilisation of urine output and urinary electrolyte excretion (Stechman *et al.*, 2010). However, mice housed in metabolic cages have been reported to display HPA axis activation (manifesting as elevated faecal excretion of corticosterone) that is sustained for up to 3 weeks (Kalliokoski *et al.*, 2013). Such an effect may have masked subtle differences in corticosterone excretion and renal fluid-electrolyte metabolism between the Hsd11b1$^{-/-}$ and control groups. However, there were no differences between these groups in basal urinary Na$^+$ excretion (measured as $U_{Na}V$ or FE_{Na}) in our renal clearance study – i.e. in mice that were not subject to the stress of a metabolic cage.

Renal electrolyte excretion: glomerular and tubular functions and molecular pathways

Glucocorticoids are known to increase renal blood flow and glomerular filtration rate (Hunter *et al.*, 2014*b*). There was a trend towards a reduction in both parameters in Hsd11b1$^{-/-}$ mice, but this did not reach statistical significance.

It is possible that, even without any change in net urinary Na$^+$ excretion, there was a change in the predominant site of Na$^+$ reabsorption in the renal tubule. For example, glucocorticoid-mediated increases in Na$^+$ reabsorption in the distal tubule might be offset by a reduction in reabsorption in the proximal tubule. We therefore assessed molecular surrogates for Na$^+$ transport activity in the thick ascending loop of Henle (NKCC2 protein expression) and the DCT (NCC protein expression and phosphorylation). These targets were chosen because their expression / activity are stimulated by glucocorticoids in rodent models (Mu *et al.*, 2011; Frindt & Palmer, 2012). We also assessed gross renal structure; glucocorticoid treatment can induce segment-specific changes in epithelial structure in the distal renal tubule of rabbits (Wade *et al.*, 1979).

We found no differences in gross renal structure, and no difference in the expression and / or phosphorylation status of NKCC2 and NCC in Hsd11b1$^{-/-}$ mice, arguing against a shift in the distribution of renal Na$^+$ transport along the nephron. However, our renal clearance study did provide some evidence of altered electrolyte transport in the distal nephron. Thiazide treatment elicited a kaliuresis of greater magnitude in Hsd11b1$^{-/-}$ mice. Thiazides stimulate K$^+$ excretion because their action delivers a tubular Na$^+$ load to the connecting tubules and collecting ducts, where Na$^+$ reabsorption through ENaC generates a lumen-negative potential gradient that drives K$^+$ secretion. We found no evidence of enhanced ENaC activity in Hsd11b1$^{-/-}$ mice: the natriuretic effect of benzamil was no greater than in wild-type mice and the proteolytic activation of ENaC-γ was not evident on Western blot. Thus we presume that the enhanced kaliuresis observed in Hsd11b1$^{-/-}$ mice reflects the activity of either ROMK or the Na-K-ATPase in the distal nephron (although we have no data to support this contention). Both of these molecules might be expected to be upregulated by the mineralocorticoid activity of DOC, which we detected at elevated levels in Hsd11b1$^{-/-}$ mice.

NDGR1 phosphorylation in whole kidney homogenates (an index of Sgk1 activation) was no different in Hsd11b1$^{-/-}$ mice. Sgk1 is a target of both mineralocorticoid (Chen *et al.*, 1999) and glucocorticoid (Hunter *et al.*, 2014*b*) signalling in renal tissue. Our finding suggest that there is no significant net stimulation of corticosteroid-responsive pathways in the kidneys of Hsd11b1$^{-/-}$ mice, but does not preclude relative differences in glucocorticoid or mineralocorticoid signalling in defined regions of the kidney.

Our failure to detect a striking water-electrolyte phenotype is in accordance with the known effects of glucocorticoids on renal tubular Na^+ transport. Glucocorticoids can stimulate Na^+ reabsorption via a number of pathways in the proximal and distal renal tubule, but their effects are often only evident when glucocorticoids are present in excess and they tend to modulate transport processes that are under the dominant control of another system (e.g. the RAAS and / or sympathetic nervous system) (Hunter *et al.*, 2014*b*). It is possible that any effect is masked by a compensatory increase in corticosterone excretion in the global Hsd11b1 knockout, and it would be interesting to examine renal Na^+ transport in a kidney-specific knockout. It is also possible that glucocorticoids only exert significant effects on renal Na^+ transport when they are present in excess. Thus, loss of renal 11βHSD1 may not yield a discernible phenotype, whereas 11βHSD1 over-expression might.

Perspective: implications for clinical medicine

Excess glucocorticoids cause obesity, insulin resistance, diabetes mellitus, hyperlipidaemia and hypertension. These traits, collectively the “metabolic syndrome”, are major risk factors for cardiovascular morbidity and mortality. Adverse cardiometabolic consequences may also be associated with “replacement” doses of therapeutic glucocorticoid, perhaps because these perturb ultradian rhythms in glucocorticoid signalling (Henley & Lightman, 2014).

The actions of 11βHSD1 in liver and adipose tissue have been extensively studied. Over-expression at these sites gives rise to salt-sensitive hypertension and activation of the renin-angiotensin-aldosterone system (Masuzaki *et al.*, 2003; Paterson *et al.*, 2004). There is an emerging hypothesis that 11βHSD1 over-activity is central to the pathogenesis metabolic syndrome (Anagnostis *et al.*, 2009) and a corresponding interest in 11βHSD1 inhibitors as therapeutic agents in the metabolic syndrome and type 2 diabetes mellitus (Tahrani *et al.*, 2011; Anagnostis *et al.*, 2013). However, the potential contribution of renal 11βHSD1 to the pathogenesis of Na$^+$-retention and hypertension in the metabolic syndrome has not – to our knowledge – been hitherto explored; nor have the potential consequences of renal 11βHSD1 inhibition. Our results suggest that renal 11βHSD1 deficiency does not exert significant effects on systemic blood pressure and Na$^+$ homeostasis. The clinical use of 11βHSD1 inhibitors would not therefore be predicted to confer significant off-target effects on renal Na$^+$ transport. No such adverse effects were detected in a clinical trial of 11βHSD1 inhibition in type 2 diabetes mellitus (Rosenstock *et al.*, 2010).

Conclusions and implications for basic renal physiology

We found no physiologically significant effect of global 11βHSD1 deletion on renal Na$^+$ excretion, arterial blood pressure, kidney function or renal perfusion. We conclude that any effect of 11βHSD1 on renal Na$^+$ excretion is subtle.

References

Ahn D, Ge Y, Stricklett PK, Gill P, Taylor D, Hughes AK, Yanagisawa M, Miller L, Nelson RD & Kohan DE (2004). Collecting duct-specific knockout of endothelin-1 causes hypertension and sodium retention. J Clin Invest 114, 504–511.

Anagnostis P, Athyros VG, Tziomalos K, Karagiannis A & Mikhailidis DP (2009). Clinical review: The pathogenetic role of cortisol in the metabolic syndrome: a hypothesis. J Clin Endocrinol Metab 94, 2692–2701.

Anagnostis P, Katsiki N, Adamidou F, Athyros VG, Karagiannis A, Kita M & Mikhailidis DP (2013). 11beta-Hydroxysteroid dehydrogenase type 1 inhibitors: novel agents for the treatment of metabolic syndrome and obesity-related disorders? Metabolism 62, 21–33.

Arriza JL, Weinberger C, Cerelli G, Glaser TM, Handelin BL, Housman DE & Evans RM (1987). Cloning of human mineralocorticoid receptor complementary DNA: structural and functional kinship with the glucocorticoid receptor. Science 237, 268–275.

Chapman K, Holmes M & Seckl J (2013). 11β-hydroxysteroid dehydrogenases: intracellular gate-keepers of tissue glucocorticoid action. Physiol Rev 93, 1139–1206.

Chen SY, Bhargava A, Mastroberardino L, Meijer OC, Wang J, Buse P, Firestone GL, Verrey F & Pearce D (1999). Epithelial sodium channel regulated by aldosterone-induced protein sgk. Proc Natl Acad Sci U S A 96, 2514–2519.

Al-Dujaili EAS, Mullins LJ, Bailey MA, Andrew R & Kenyon CJ (2009a). Physiological and pathophysiological applications of sensitive ELISA methods for urinary deoxycorticosterone and corticosterone in rodents. Steroids 74, 938–944.

Al-Dujaili E a. S, Mullins LJ, Bailey MA & Kenyon CJ (2009b). Development of a highly sensitive ELISA for aldosterone in mouse urine: validation in physiological and pathophysiological states of aldosterone excess and depletion. Steroids 74, 456–462.

Frindt G & Palmer LG (2012). Regulation of epithelial Na+ channels by adrenal steroids: Mineralocorticoid and glucocorticoid effects. Am J Physiol Renal Physiol 302, F20–F26.

Gong R, Morris DJ & Brem AS (2008). Human renal 11beta-hydroxysteroid dehydrogenase 1 functions and co-localizes with COX-2. Life Sci 82, 631–637.

Harris HJ, Kotelevtsev Y, Mullins JJ, Seckl JR & Holmes MC (2001). Intracellular regeneration of glucocorticoids by 11beta-hydroxysteroid dehydrogenase (11beta-HSD)-1 plays a key role in regulation of the hypothalamic-pituitary-adrenal axis: analysis of 11beta-HSD-1-deficient mice. Endocrinology 142, 114–120.

Henley DE & Lightman SL (2014). Cardio-metabolic consequences of glucocorticoid replacement: relevance of ultradian signalling. Clin Endocrinol (Oxf) 80, 621–628.

Hunter RW, Craigie E, Homer NZM, Mullins JJ & Bailey MA (2014a). Acute inhibition of NCC does not activate distal electrogenic Na+ reabsorption or kaliuresis. Am J Physiol Renal Physiol 306, F457–F467.

Hunter RW, Ivy JR & Bailey MA (2014b). Glucocorticoids and renal Na+ transport: implications for hypertension and salt sensitivity. J Physiol 592, 1731–1744.

Hunter RW, Ivy JR, Flatman PW, Kenyon CJ, Craigie E, Mullins LJ, Bailey MA & Mullins JJ (2014c). Hypertrophy in the Distal Convoluted Tubule of an 11β-Hydroxysteroid Dehydrogenase Type 2 Knockout Model. J Am Soc Nephrol JASN; DOI: 10.1681/ASN.2013060634.

Inglis SK, Gallacher M, Brown SG, McTavish N, Getty J, Husband EM, Murray JT & Wilson SM (2009). SGK1 activity in Na+ absorbing airway epithelial cells monitored by assaying NDRG1-Thr346/356/366 phosphorylation. Pflüg Arch Eur J Physiol 457, 1287–1301.

Kalliokoski O, Jacobsen KR, Darusman HS, Henriksen T, Weimann A, Poulsen HE, Hau J & Abelson KSP (2013). Mice do not habituate to metabolism cage housing--a three week study of male BALB/c mice. PloS One 8, e58460.

Kotelevtsev Y, Holmes MC, Burchell A, Houston PM, Schmoll D, Jamieson P, Best R, Brown R, Edwards CR, Seckl JR & Mullins JJ (1997). 11beta-hydroxysteroid dehydrogenase type 1 knockout mice show attenuated glucocorticoid-inducible responses and resist hyperglycemia on obesity or stress. Proc Natl Acad Sci U S A 94, 14924–14929.

Lavery GG, Idkowiak J, Sherlock M, Bujalska I, Ride JP, Saqib K, Hartmann MF, Hughes B, Wudy SA, De Schepper J, Arlt W, Krone N, Shackleton CH, Walker EA & Stewart PM (2013). Novel H6PDH mutations in two girls with premature adrenarche: "apparent" and "true" CRD can be differentiated by urinary steroid profiling. Eur J Endocrinol Eur Fed Endocr Soc 168, K19–K26.

Liang M, Yuan B, Rute E, Greene AS, Olivier M & Cowley AW (2003). Insights into Dahl salt-sensitive hypertension revealed by temporal patterns of renal medullary gene expression. Physiol Genomics 12, 229–237.

Liu Y, Singh RJ, Usa K, Netzel BC & Liang M (2008). Renal medullary 11 beta-hydroxysteroid dehydrogenase type 1 in Dahl salt-sensitive hypertension. Physiol Genomics 36, 52–58.

Mangos GJ, Whitworth JA, Williamson PM & Kelly JJ (2003). Glucocorticoids and the kidney. Nephrol Carlton Vic 8, 267–273.

Masilamani S, Wang X, Kim G-H, Brooks H, Nielsen J, Nielsen S, Nakamura K, Stokes JB & Knepper MA (2002). Time course of renal Na-K-ATPase, NHE3, NKCC2, NCC, and ENaC abundance changes with dietary NaCl restriction. AJP Ren Physiol 283, F648–F657.

Masuzaki H, Yamamoto H, Kenyon CJ, Elmquist JK, Morton NM, Paterson JM, Shinyama H, Sharp MGF, Fleming S, Mullins JJ, Seckl JR & Flier JS (2003). Transgenic amplification of glucocorticoid action in adipose tissue causes high blood pressure in mice. J Clin Invest 112, 83–90.

McKinnell J, Roscoe D, Holmes MC, Lloyd-MacGilp SA & Kenyon CJ (2000). Regulation of 11beta-hydroxysteroid dehydrogenase enzymes by dietary sodium in the rat. Endocr Res 26, 81–95.

Morgan SA, McCabe EL, Gathercole LL, Hassan-Smith ZK, Larner DP, Bujalska IJ, Stewart PM, Tomlinson JW & Lavery GG (2014). 11β-HSD1 is the major regulator of the tissue-specific effects of circulating glucocorticoid excess. Proc Natl Acad Sci U S A 111, E2482–E2491.

Morton NM, Paterson JM, Masuzaki H, Holmes MC, Staels B, Fievet C, Walker BR, Flier JS, Mullins JJ & Seckl JR (2004). Novel adipose tissue-mediated resistance to diet-induced visceral obesity in 11 beta-hydroxysteroid dehydrogenase type 1-deficient mice. Diabetes 53, 931–938.

Murray JT, Campbell DG, Morrice N, Auld GC, Shpiro N, Marquez R, Peggie M, Bain J, Bloomberg GB, Grahammer F, Lang F, Wulff P, Kuhl D & Cohen P (2004). Exploitation of KESTREL to identify NDRG family members as physiological substrates for SGK1 and GSK3. Biochem J 384, 477–488.

Mu S, Shimosawa T, Ogura S, Wang H, Uetake Y, Kawakami-Mori F, Marumo T, Yatomi Y, Geller DS, Tanaka H & Fujita T (2011). Epigenetic modulation of the renal β-adrenergic-WNK4 pathway in salt-sensitive hypertension. Nat Med 17, 573–580.

Odermatt A & Kratschmar DV (2012). Tissue-specific modulation of mineralocorticoid receptor function by 11 beta-hydroxysteroid dehydrogenases: An overview. Mol Cell Endocrinol 350, 168–186.

Paterson JM, Morton NM, Fievet C, Kenyon CJ, Holmes MC, Staels B, Seckl JR & Mullins JJ (2004). Metabolic syndrome without obesity: Hepatic overexpression of 11beta-hydroxysteroid dehydrogenase type 1 in transgenic mice. Proc Natl Acad Sci U S A 101, 7088–7093.

Rosenstock J, Banarer S, Fonseca VA, Inzucchi SE, Sun W, Yao W, Hollis G, Flores R, Levy R, Williams WV, Seckl JR, Huber R & INCB13739-202 Principal Investigators (2010). The 11-beta-hydroxysteroid dehydrogenase type 1 inhibitor INCB13739 improves hyperglycemia in patients with type 2 diabetes inadequately controlled by metformin monotherapy. Diabetes Care 33, 1516–1522.

Stechman MJ, Ahmad BN, Loh NY, Reed AAC, Stewart M, Wells S, Hough T, Bentley L, Cox RD, Brown SDM & Thakker RV (2010). Establishing normal plasma and 24-hour urinary biochemistry ranges in C3H, BALB/c and C57BL/6J mice following acclimatization in metabolic cages. Lab Anim 44, 218–225.

Tahrani AA, Bailey CJ, Del Prato S & Barnett AH (2011). Management of type 2 diabetes: new and future developments in treatment. Lancet 378, 182–197.

Wade JB, O'Neil RG, Pryor JL & Boulpaep EL (1979). Modulation of cell membrane area in renal collecting tubules by corticosteroid hormones. J Cell Biol 81, 439–445.

Additional information

Competing interests

None declared.

Author contributions

Conception and design of the experiments: THC, RWH, CJK, BLJ, MAB

Collection, analysis and interpretation of data: THC, RWH, CJK, MAB

Drafting the article or revising it critically for important intellectual content: THC, RWH, CJK, BJL, MAB

Funding

THC received funding from the Lundbeck foundation (Lundbeckfonden; grant number R152-2013-14574) and the Danish Agency for Higher Education. This work was also funded by Kidney Research UK (grant number IN11/2011). RWH is employed as a clinical lecturer on the ECAT scheme by the University of Edinburgh.

Acknowledgments

We thank Jessica Ivy and Audrey Peter (Centre for Cardiovascular Science, University of Edinburgh) for their assistance in performing some of the experimental assays, Ruth Hamblin (Immunodetection CoRE, Queen's Medical Research Institute, University of Edinburgh) for performing the immunohistochemical stains and Mette Stæhr (Department of Cardiovascular and Renal Research, University of Southern Denmark, Odense, Denmark) for the generous provision of the low Na^+ diet. We are very grateful to Professor Johannes Loffing (Zurich Center of Integrative Human Physiology, University of Zurich, Switzerland) for the generous provision of antibodies to ENaC-γ.

Table 1. Baseline characteristics of experimental cohorts. Data presented as mean ± standard deviation. Comparisons between genotypes are by unpaired t-tests; significant p-values are underlined.

cohort	**n =**	**age** */ days*	**body weight** */ g*	**kidney weight** */ mg*	**kidney:BW ratio** */ mg per g*
Metabolic study: high Na$^+$ group					
WT	11	81 ± 3.3	25.0 ± 1.4	160.9 ± 9.9	6.65 ± 0.41
Hsd11b1$^{-/-}$	11	91 ± 11.4	27.7 ± 2.5	172.9 ± 13.5	6.88 ± 0.88
p =			*0.006*	*0.027*	*0.438*
Metabolic study: low Na$^+$ group					
WT	6	97 ± 3.7	26.8 ± 2.7	156.5 ± 9.3	6.41 ± 0.55
Hsd11b1$^{-/-}$	6	103 ± 12.0	31.1 ± 3.5	190.5 ± 22.2	6.54 ± 0.44
p =			*0.040*	*0.006*	*0.647*
Renal clearance study: effect of bendroflumethiazide					
WT	7	214 ± 82.5	33.9 ± 5.0	173.5 ± 19.3	5.16 ± 0.44
Hsd11b1$^{-/-}$	8	164 ± 65.9	34.2 ± 6.4	179.0 ± 17.3	5.34 ± 0.84
p =			*0.912*	*0.574*	*0.620*
Renal clearance study: effect of benzamil					
WT	6	126 ± 2.7	31.4 ± 1.7	304.7 ± 35.2	9.68 ± 0.78
Hsd11b1$^{-/-}$	5	101 ± 9.9	29.2 ± 1.1	276.6 ± 14.7	9.46 ± 0.46
p =			*0.037*	*0.132*	*0.594*
Histology study					
WT	3	174 ± 1.5	30.7 ± 3.3		
Hsd11b1$^{-/-}$	3	191 ± 0.6	31.7 ± 1.0		
p =			*0.631*		

A

		WT	**Hsd11b1 $^{-/-}$**	*p*
P_{Na}	*mM*	146.6 ± 2.4	148.1 ± 2.7	*0.2604*
P_{K}	*mM*	3.69 ± 0.28	3.50 ± 0.35	*0.2785*
P_{Cl}	*mM*	118.3 ± 3.5	118.6 ± 4.7	*0.8794*
Hct	*%*	42.0 ± 2.4	40.9 ± 2.5	*0.3876*

B

	BASELINE		**BFTZ**		**p-values**		
	WT	**Hsd11b1 $^{-/-}$**	**WT**	**Hsd11b1 $^{-/-}$**	**BFZ**	**GT**	**IA**
UV $\mu L \cdot min^{-1} \cdot g\ KW^{-1}$	7.54 (5.34 , 9.75)	5.42 (3.15 , 7.96)	30.44 (19.62 , 41.26)	32.81 (23.70 , 41.91)	*<0.0001*	*0.9651*	*0.5028*
$U_{Na}V$ $\mu mol \cdot min^{-1} \cdot g\ KW^{-1}$	0.68 (-0.01 , 1.38)	0.59 (0.17 , 1.01)	7.06 (4.02 , 10.09)	7.64 (5.16 , 10.12)	*<0.0001*	*0.7687*	*0.6895*
$U_{K}V$ $\mu mol \cdot min^{-1} \cdot g\ KW^{-1}$	1.77 (1.10 , 2.44)	1.17 (0.78 , 1.55)	2.24 (1.71 , 2.78)	2.74 (2.06 , 3.43)	*0.0012*	*0.8279*	*0.0435*
$U_{Cl}V$ $\mu mol \cdot min^{-1} \cdot g\ KW^{-1}$	0.57 (-0.08 , 1.21)	0.37 (0.19 , 0.54)	5.24 (2.83 , 7.64)	5.55 (3.80 , 7.29)	*<0.0001*	*0.9352*	*0.6612*
FE_{K} *%*	42.8 (33.6 , 52.1)	41.1 (33.9 , 48.2)	57.2 (40.8 , 73.6)	68.0 (56.0 , 80.1)	*0.0002*	*0.4161*	*0.1515*
FE_{Cl} *%*	0.38 (0.03 , 0.74)	0.40 (0.22 , 0.58)	3.63 (2.59 , 4.67)	3.89 (2.97 , 4.67)	*<0.0001*	*0.6624*	*0.6702*

Table 2. Renal clearance data. Hsd11b1$^{-/-}$ (n = 8) and wild-type (n = 7) mice were used in a renal clearance study as described in the main text. **A)** Plasma electrolyte concentrations and haematocrit (HCT) in the terminal blood sample. Data are presented as mean ± SD. There were no significant differences between genotypes (by unpaired t-test). **B)** Renal clearance parameters at baseline and following a bolus dose of bendroflumethiazide (BFTZ). Data are presented as mean and 95 % CI. UV, urine flow; $U_{Na}V$, $U_{K}V$ and $U_{Cl}V$, urinary excretion of Na^+, K^+ and Cl^-; FE_{K} and FE_{Cl}, fractional excretion of K^+ and Cl^-. p-values for comparisons between genotypes (GT) and baseline vs. after BFTZ made by 2-way ANOVA with repeated measures; IA = interaction. p-values < 0.05 are underlined.

Figure 1. Experimental protocols. A) Time-course of experimental protocols for balance studies. **B)** Time-course of renal clearance studies. P1, P2, P3: plasma collections. BFTZ: bendroflumethiazide 2 mg per kg body weight administered as an intravenous bolus. BZM: benzamil 2 mg per kg body weight administered as an intravenous bolus. (NB BFTZ and BZM were used in separate experimental series; they were never administered together.)

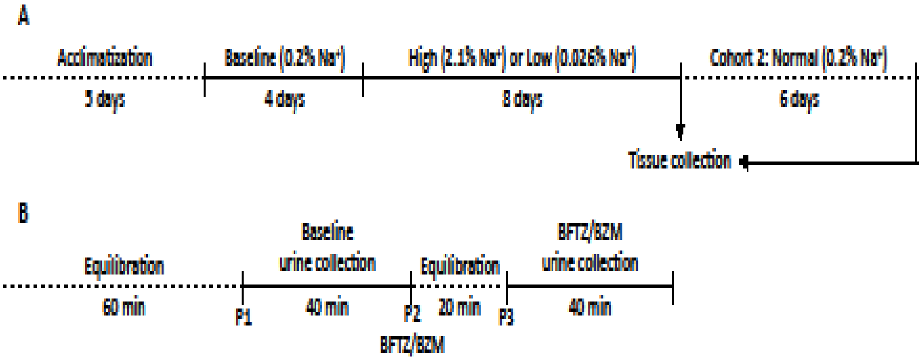
A
Acclimatization
5 days
Baseline (0.2% Na⁺)
4 days
High (2.1% Na⁺) or Low (0.026% Na⁺)
8 days
Cohort 2: Normal (0.2% Na⁺)
6 days
Tissue collection
B
Equilibration
60 min
P1
Baseline
urine collection
40 min
P2
BFTZ/BZM
Equilibration
20 min
P3
BFTZ/BZM
urine collection
40 min

Figure 2. Water, sodium and potassium balance in Hsd11b1$^{-/-}$ and wild-type and mice. Dietary intake and urinary and faecal excretion of water, Na^+ and K^+ were measured in metabolic cages. Balance data were calculated as the difference between dietary intake and total excretion (sum of urinary and faecal excretion). All data were normalised to kidney weight (KW). Mice were fed a baseline (0.2 % Na^+) diet for four days, followed by high Na^+ (2.1 %) or low Na^+ (0.026 %) diet for eight days. **A – C)** Response to high-Na^+ diet (n = 11 Hsd11b1$^{-/-}$ + 11 wild-type). **D – F)** Response to low-Na^+ diet (n = 6 + 6). Data are presented as mean ± 95 % CI. Comparisons between genotype (GT) and sodium intake (SI) were made by 2-way ANOVA; IA = interaction. * $p < 0.05$ by *post hoc* Holm-Šídák test.

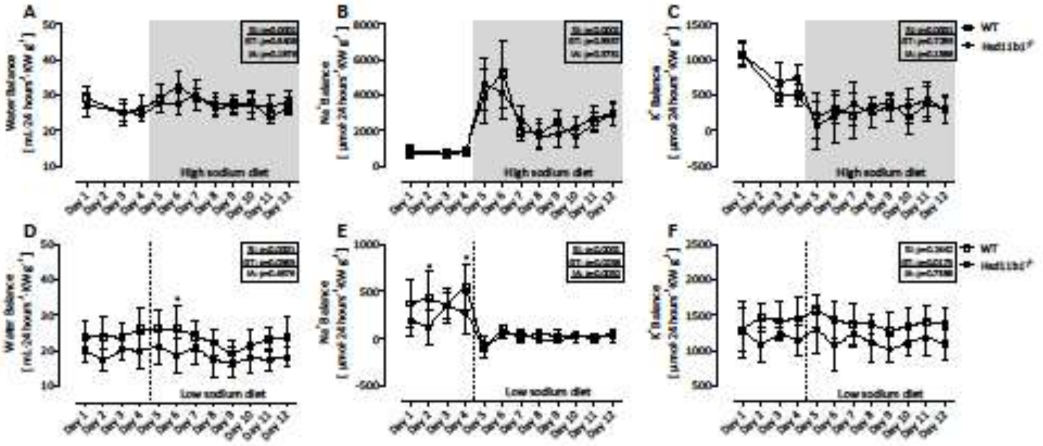

Figure 3. Renal clearance data: effect of bendroflumethiazide. Hsd11b1$^{-/-}$ (n = 8) and wild-type (n = 7) mice were used in a renal clearance study as described in the main text. Recordings were made during a baseline period and after the intravenous administration of bendroflumethiazide (BFTZ), 2 mg per kg body weight. **A)** Mean arterial blood pressure, MABP. **B)** Renal blood flow, RBF. **C)** Glomerular filtration rate, GFR. **D)** Fractional excretion of Na$^+$, FE$_{Na}$. Data are presented as mean ± 95 % CI. Comparison between genotypes (GT) and baseline vs. after BFTZ were made by 2-way ANOVA with repeated measures; IA = interaction. There were no significant differences between genotypes.

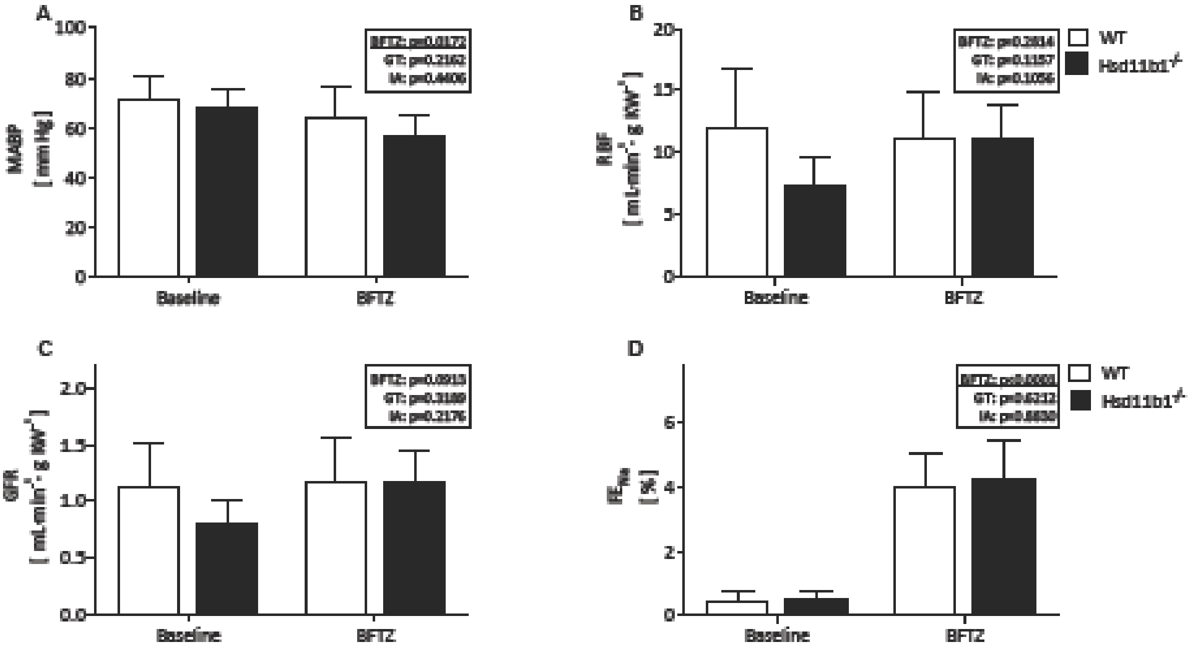

Figure 4. Renal clearance data: effect of benzamil. The natriuretic effect of benzamil (BZM) was tested in a renal clearance study. BZM was administered intravenously at a dose of 2 mg per kg body weight to Hsd11b1$^{-/-}$ (n = 5) and wild-type (n = 6) mice. The fractional excretion of Na$^+$ (FE$_{Na}$) was determined before and after BZM. Data are presented as mean ± 95 % CI. Comparison between genotypes (GT) and baseline vs. after BZM were made by 2-way ANOVA with repeated measures; IA = interaction. There were no significant differences between genotypes.

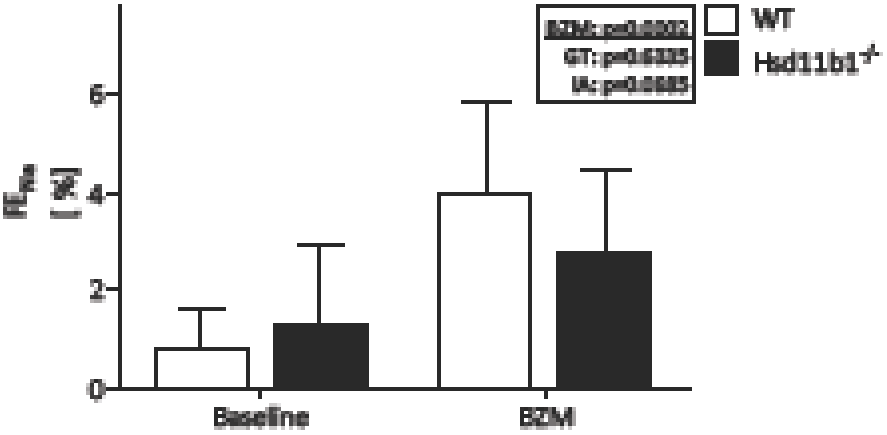

Figure 5. Longitudinal urinary steroid excretion. A & D) Urinary corticosterone excretion in response to high- and low-Na$^+$ diet respectively (n = 3 Hsd11b1$^{-/-}$ + 3 wild-type). **B & E)** Urinary aldosterone excretion on high- and low-Na$^+$ diet respectively (n = 3 + 3). **C & F)** Urinary DOC excretion on high- and low-Na$^+$ diet respectively (n = 3 + 3). Data are presented as mean ± 95% CI. Comparisons between genotype (GT) and sodium intake (SI) were made by 2-way ANOVA with repeated measures; IA = interaction. * $p < 0.05$ between genotypes by *post hoc* Holm-Šídák test. (Aldosterone results were missing for day 4 on high Na$^+$ and day 11 on low Na$^+$; these data were excluded from the ANOVA.)

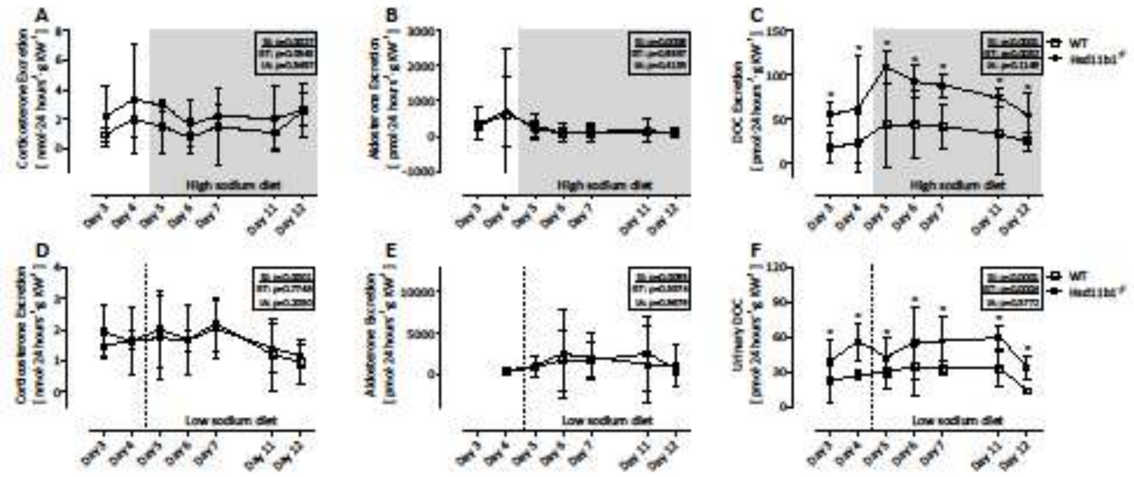

Figure 6. Cross-sectional area of adrenal cells in Hsd11b1$^{-/-}$ and wild-type mice. Adrenal glands were harvested from Hsd11b1$^{-/-}$ and wild-type mice maintained on normal- (0.2 %) and low- (0.026 %) Na^+ diets for 8 days. Mean cell size was measured in **A)** the zona glomerulosa of the adrenal cortex; **B)** outer zona fasciculata; **C)** inner zona fasciculata and **D)** the adrenal medulla. Data are presented as mean ± 95 % CI. Comparison between genotype (GT) and sodium intake (SI) were made by 2-way ANOVA; IA = interaction. **E) – H)** Representative images of adrenal sections, stained with haematoxylin and eosin. Scale-bars are 100 microns.

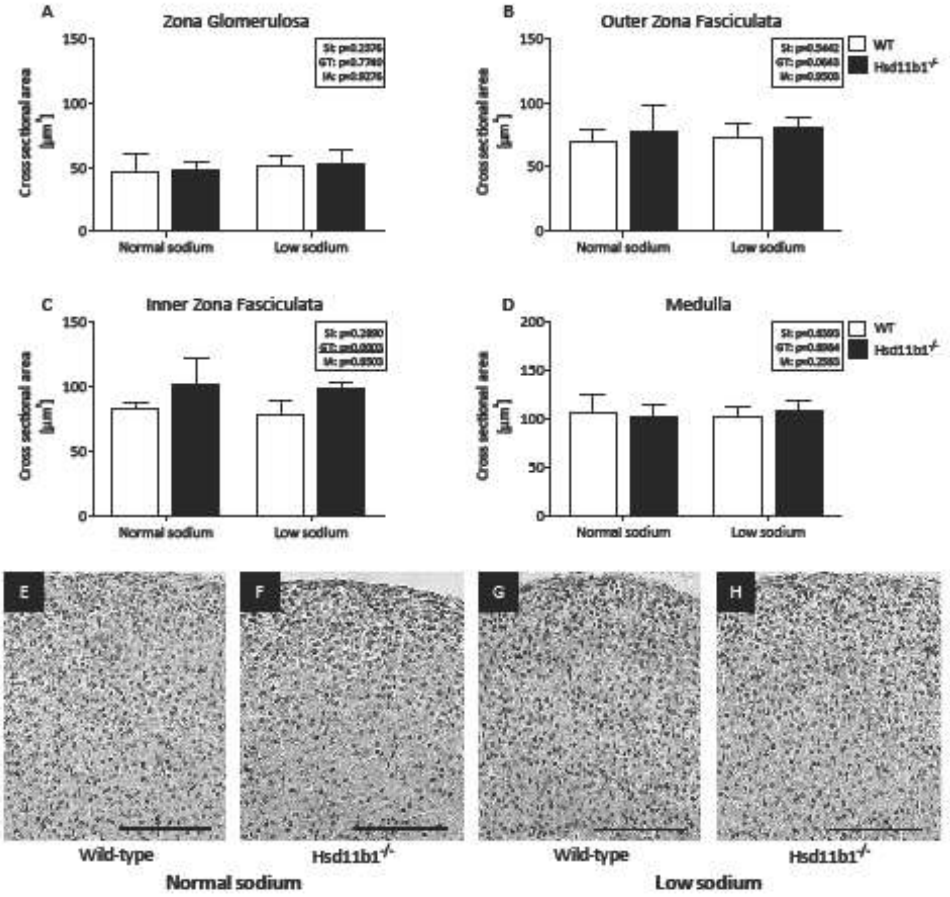

Figure 7. Activity of renin-angiotensin and nitric oxide systems. A) Plasma renin concentration in Hsd11b1$^{-/-}$ mice on normal (n = 9) and high (n = 5) Na^+ diet and wild-type mice on normal (n = 13) and high (n = 5) Na^+ diet. **B)** Plasma angiotensinogen concentration in the same experimental groups (n = 8, 4, 10 and 4 respectively). **C & D)** Urinary NO_x excretion (representative of total body NO production) in Hsd11b1$^{-/-}$ and wild-type mice on high and low Na^+ diet respectively (n = 5 for each experimental group). Data are presented as mean ± 95 % CI. Comparison between genotype (GT) and sodium intake (SI) were made by 2-way ANOVA; IA = interaction.

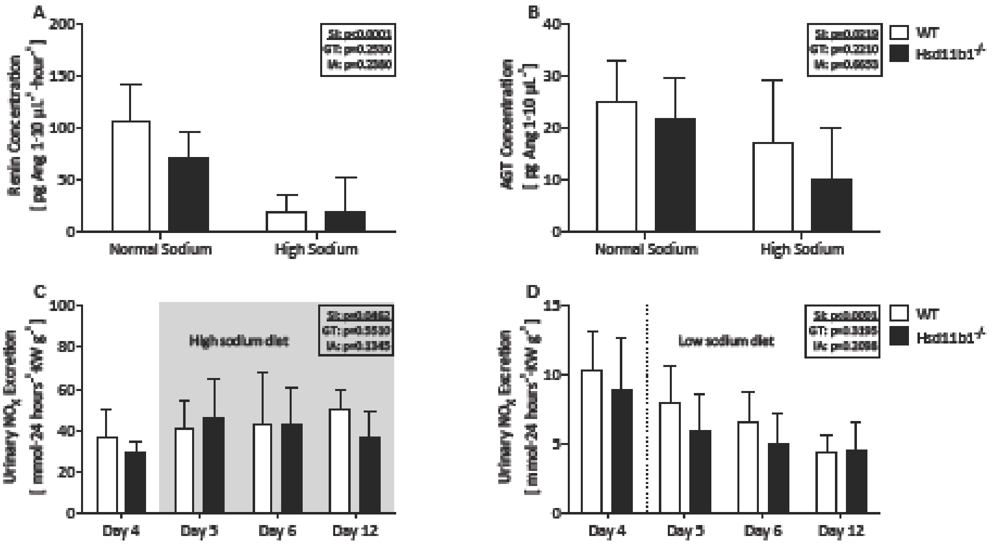

Figure 8. Renal histology and NCC expression by immunohistochemistry. A & B) Renal cortex (H&E stain) in wild-type and Hsd11b1$^{-/-}$ mice respectively. No gross changes in renal histology were apparent in Hsd11b1$^{-/-}$ mice (n = 3 for each genotype); representative images are shown. **C & D)** Low-power view of immunohistochemical stain for NCC in renal cortex of wild-type and Hsd11b1$^{-/-}$ mice respectively. **E & F)** High-power view of immunohistochemical stain for NCC in renal cortex of wild-type and Hsd11b1$^{-/-}$ mice respectively. NCC was detected (as expected) in the apical cell membrane of the distal convoluted tubule. The distribution did not differ between genotypes (n = 3 + 3); representative images are shown.

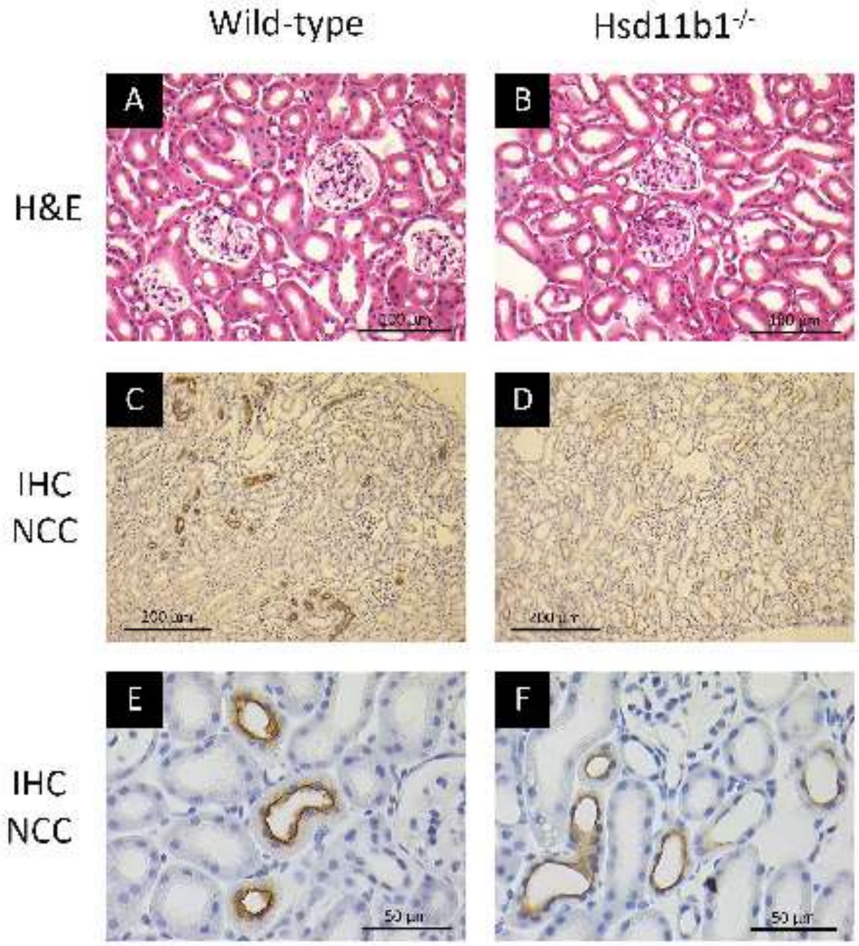
Wild-type
Hsd11b1-/-
H&E
A
100 μm
B
100 μm
IHC NCC
C
200 μm
D
200 μm
IHC NCC
E
50 μm
F
50 μm

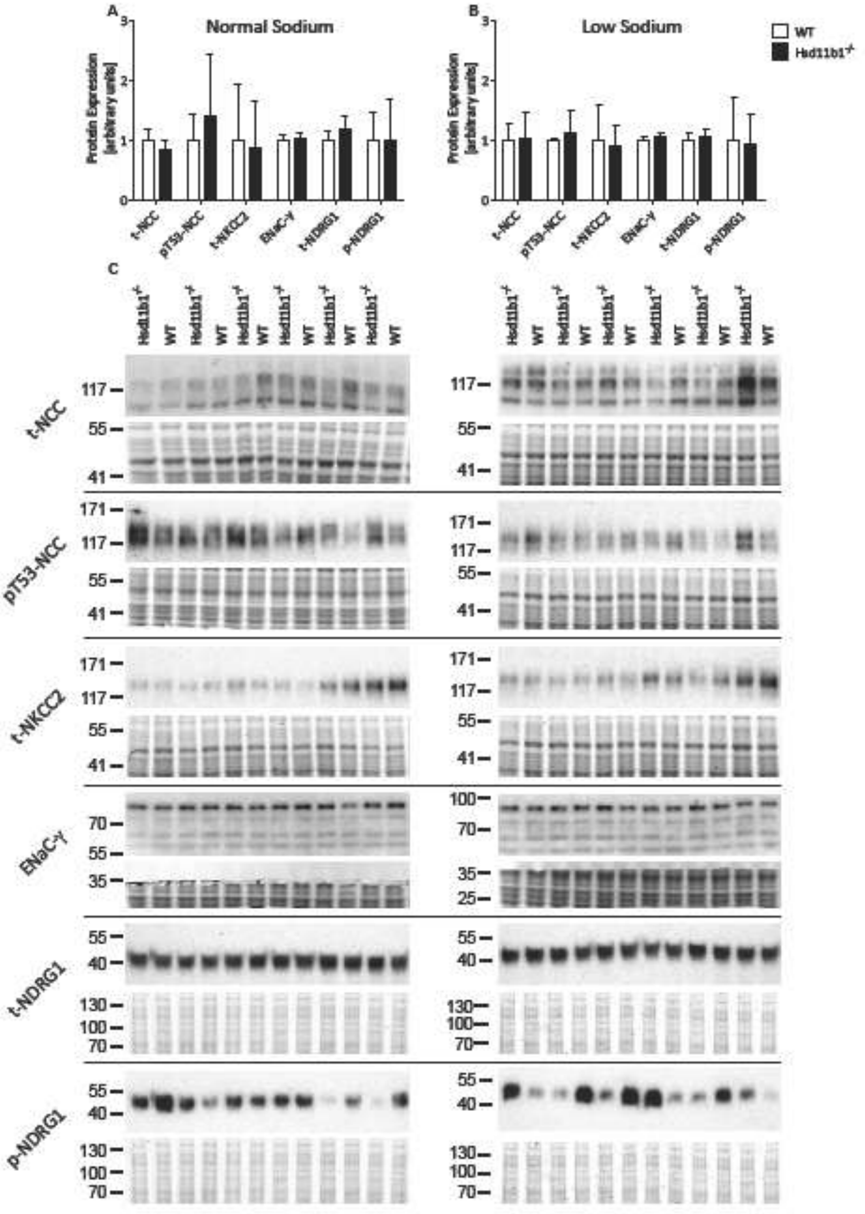Figure 9. Immunoblot analysis in whole kidney homogenates from Hsd11b1$^{-/-}$ and wild-type mice. **A)** Densitometry analysis of immunoblots for total NCC (t-NCC), the phosphorylated form pT53-NCC, NKCC2 (t-NKCC2), ENaC-γ and total (t-) and phosphorylated (p-) NDRG1. Whole kidney homogenates were prepared from Hsd11b1$^{-/-}$ (n = 6) and wild-type mice (n = 6) maintained on normal (0.2 %) Na^+ diet (cohort 2 from the metabolic study). After correction with a loading control (Coomassie-stained band), density was normalised so that for each target protein, the wild-type group had a mean density of 1.0. For ENaC-γ, densitometry data are presented for the sum of all bands. **B)** Densitometry analysis applied to immunoblots of kidney homogenates from mice maintained on a low (0.026 %) Na^+ diet (n = 6 for each genotype). Data are presented as mean ± 95 % CI. There were no significant differences between genotypes in either the normal or the low Na^+ cohort (by unpaired t-test). No inferences were drawn between blots – i.e. between normal and low-Na^+ groups. **C)** Representative immunoblots; the Coomassie-stained gel used as a loading control is shown below each blot. Size markers are in kDa.